SUPPLEMENTAL MATERIAL

SENP1 promotes hypoxia-induced cancer stemness by HIF-1α deSUMOylation and SENP1/HIF-1α positive feedback loop

Chun-Ping Cui [1,4], Carmen Chak-Lui Wong [1,3], Alan Ka-Lun Kai [1], Daniel Wai-Hung Ho [1,3], Eunice Yuen-Ting Lau [1,5], Yu-Man Tsui [1,3], Tan-To Cheung [2,3], Kenneth Siu-Ho Chok [2,3], Albert C.Y. Chan [2,3], Regina Cheuk-Lam Lo [1,3], Joyce Man-Fong Lee [1], Terence Kin-Wah Lee [1,3.5], Irene Oi Lin Ng[1,3,#]

[1]Departments of Pathology and [2]Surgery and [3]State Key Laboratory for Liver Research, The University of Hong Kong, Queen Mary Hospital, Pokfulam, Hong Kong.

[4]State Key Laboratory of Proteomics, Beijing Proteome Research Center, Beijing Institute of Radiation Medicine, 27 Taiping Road, Beijing 100850, China.

[5]Current address: Department of Applied Biology and Chemical Technology, The Hong Kong Polytechnic University, Hong Kong.

Supplemental figures

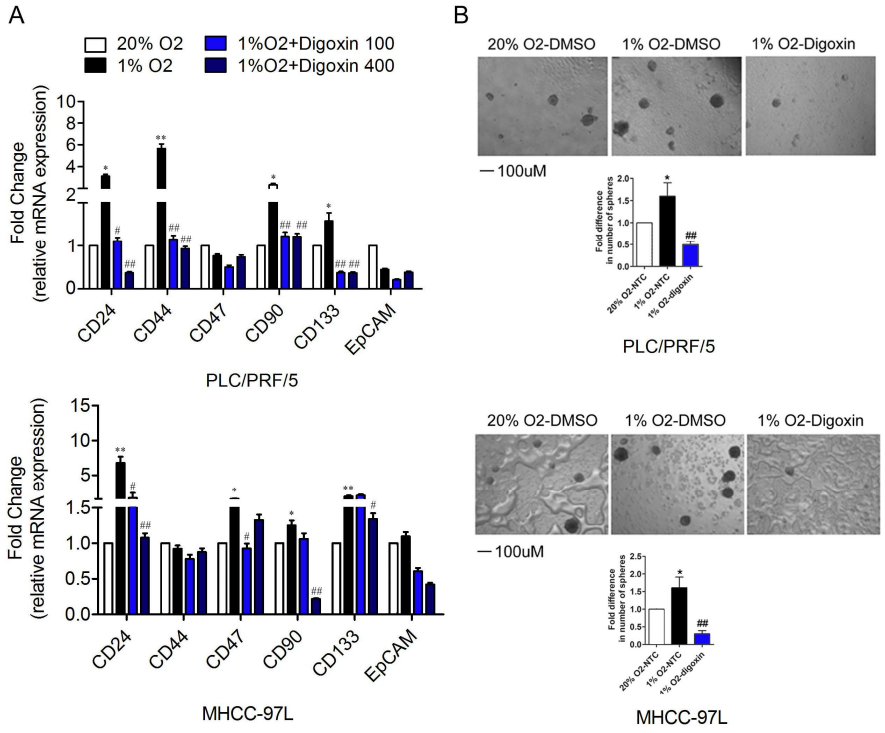

Figure S1. Hypoxia induced the expression of CSC markers and enhanced self-renewal ability in PLC/PRF/5 and MHCC-97L cells. (A) Expression of CD24, CD44, CD47, CD90, CD133 and EpCAM at mRNA levels in HCC cells under hypoxia and normoxia and with digoxin at the concentrations of 100nM and 400nM. (B) Self-renewal ability was assessed by sphere formation assay in HCC cells under hypoxia and normoxia and with digoxin at the concentration of 100nM. (*$p < 0.05$, **$p < 0.01$, as compared with the negative control in normoxia [20% O2]; $^{\#}p < 0.05$, $^{\#\#}p < 0.01$, as compared with the vehicle control in hypoxia [1% O_2]).

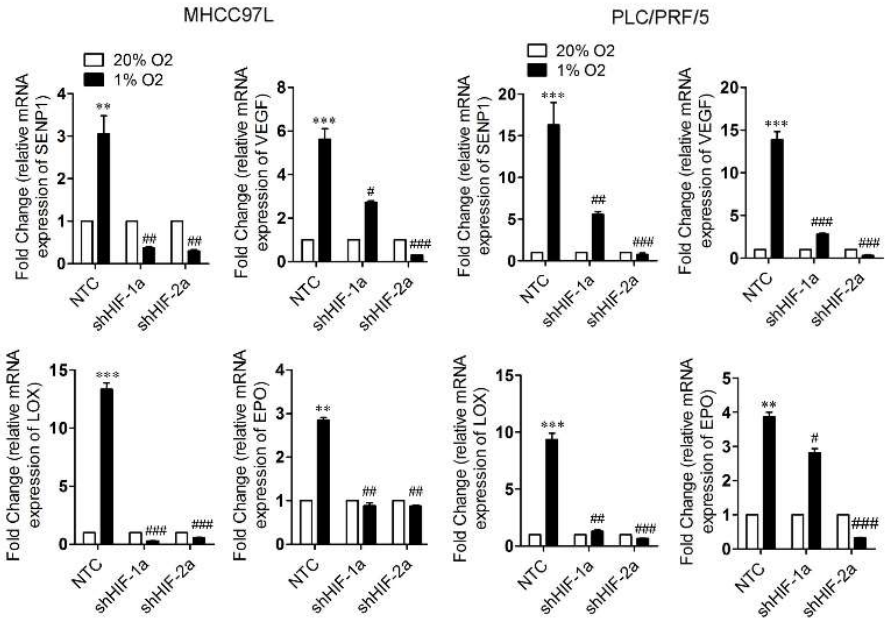

Figure S2. Expression of SENP1, VEGF, LOX and EPO at mRNA levels in two HCC cell lines (MHCC-97Land PLC/PRF/5) with stable knockdown of HIF-1α, HIF-2α or NTC under hypoxic and normoxic condition. (*p< 0.05, **p < 0.01, ***p < 0.001, as compared with the negative control in normoxia [20% O_2]; $^{\#}$p < 0.05, $^{\#\#}$p < 0.01, $^{\#\#\#}$p < 0.001, as compared with the vehicle control in hypoxia [1% O_2]).

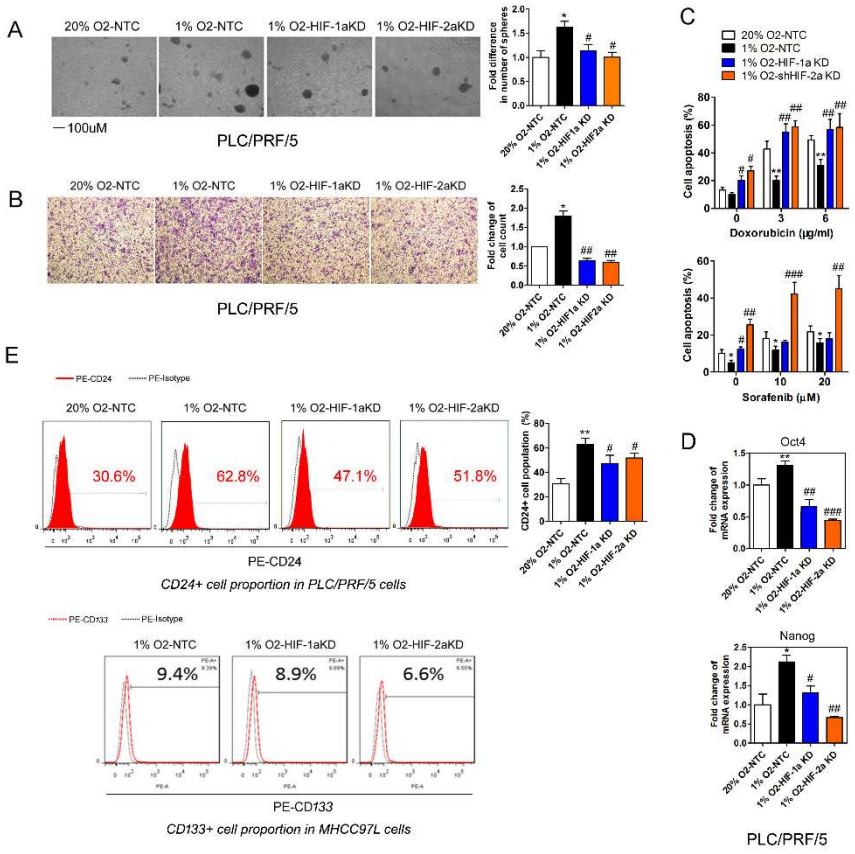

Figure S3. HIF-1/2α knockdown suppressed the hypoxia-induced effects on stemness of HCC cells. (A-C) The *in vitro* abilities of self-renewal (A), migration (B) and chemoresistance (C) were enhanced under hypoxic condition (1% O_2) in PLC/PRF/5 cells. Knockdown of HIF-1α or HIF-2α suppressed these hypoxia-induced effects. (D) Hypoxia-induced increase in mRNA expression of stemness-related genes (Oct3/4, Nanog) was inhibited in HIF-1α or HIF-2α knockdown PLC/PRF/5 cells. (E) $CD24^+$ cell populations were increased in hypoxia-treated PLC/PRF/5 cells, but the knockdown of HIF-1α or HIF-2α blunted the effect (upper panel) (*$p < 0.05$, **$p < 0.01$, ***$p < 0.001$, as compared with the negative control in normoxia [20% O_2]; $^{\#}p < 0.05$, $^{\#\#}p < 0.01$, $^{\#\#\#}p < 0.001$, as compared with the vehicle control in hypoxia [1% O_2]). Similar but milder trend was seen for the $CD133^+$ cell population in MHCC-97L cells in hypoxia with knockdown of HIF-1α or HIF-2α (lower panel).

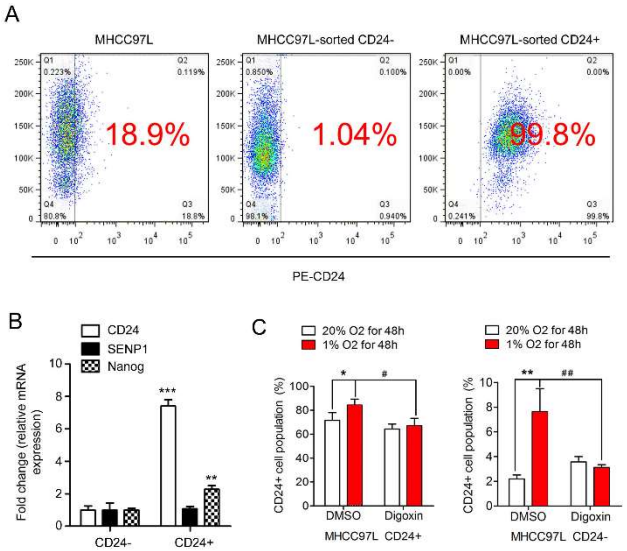

Figure S4. (A) Percentage of $CD24^+$ cell population in sorted $CD24^+$ and $CD24^-$ cells in MHCC-97L. (B) CD24, Nanog, and SENP1 mRNA level in sorted $CD24^+$ and $CD24^-$ MHCC-97L cells. (C) Digoxin, a HIF-α inhibitor, suppressed the maintenance of CD24 in sorted $CD24^+$ (left) under hypoxic or normoxic condition and the induction of $CD24^+$ cells under hypoxia in the $CD24^-$ (right) cells (*$p < 0.05$, **$p < 0.01$, ***$p < 0.001$, as compared with the $CD24^-$ HCC cells or the vehicle control).

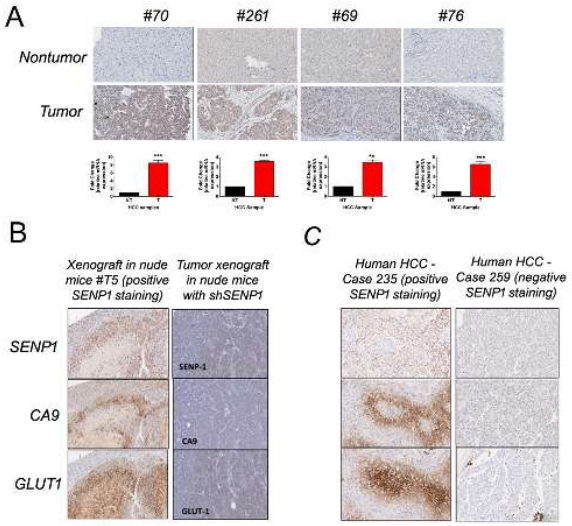

Figure S5. (A) Consistent with the results of qPCR, higher expression of SENP1 at protein level was observed in paraffin-embedded tumor tissues by IHC (*p < 0.05, **p < 0.01, ***p < 0.001, as compared with NT). (B) Using immunohistochemistry, we observed a good correlation among the expression of two HIF-1α-dependent genes, carbonic anhydrase 9 (CA9) and glucose transporter 1 (GLUT1), and SENP1 in mouse HCC xenograft (S5B). In addition, much reduced expression of CA9 and GLUT1 was seen in the shSENP1 cells in HCC xenografts. (C) Similarly good correlation was seen among CA9, GLUT1, and SENP1 expression in human HCCs tissues. The human HCC case with good expression of SENP1 had strong expression of CA9 and GLUT1 (left panel), whereas the other human HCC case with minimal expression of SENP1 had weak expression of CA9 and GLUT1 (right panel).

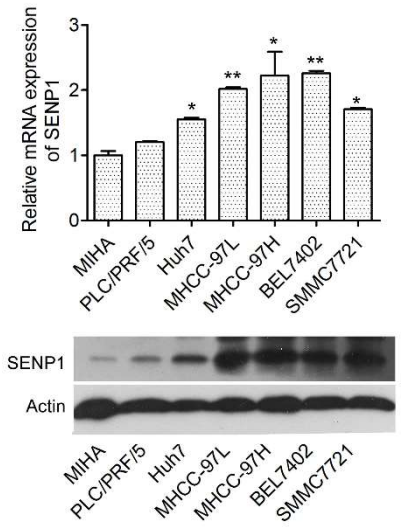

Figure S6. Basic levels of SENP1 mRNA and protein in human immortalized normal liver cells and different HCC cell lines, as detected with q-PCR and western blotting.

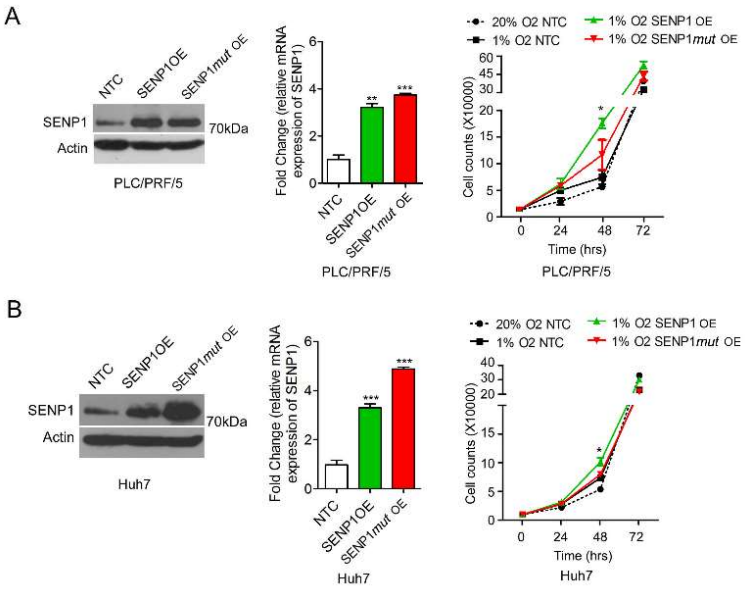

Figure S7. (A) Q-PCR and western blots were used to examine the efficiency of stable SENP1 overexpression in PLC/PRF/5 cells. Cell proliferation assay showed SENP1 overexpression enhanced cell growth in PLC/PRF/5 cells. (B) Q-PCR and western blots were used to examine the efficiency of stable SENP1 overexpression in Huh7 cells. Cell proliferation assay showed SENP1 overexpression enhanced Huh7 cell growth in vitro. (*p < 0.05, **p < 0.01, ***p < 0.001, as compared with the negative control).

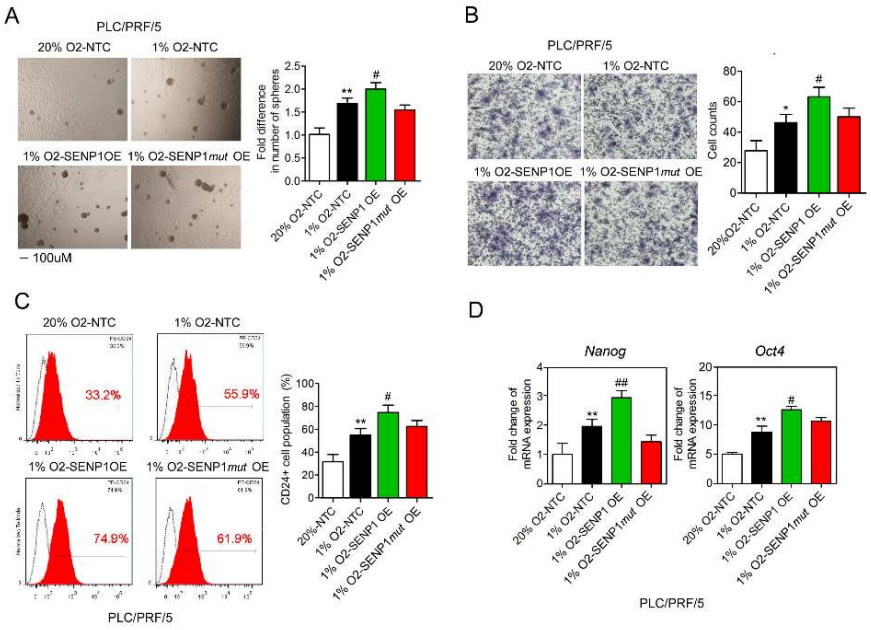

Figure S8. SENP1 overexpression enhanced the stemness of PLC/PRF/5 cells. The effects of overexpression of SENP1, SENP1mut and NTC on the stemness of HCC cells as shown by abilities of self-renewal (A) and cell migration (B), $CD24^+$ cell population (C), and mRNA expression of stemness-related genes (D) in hypoxic condition. (*$p < 0.05$, **$p < 0.01$, as compared with the negative control in normoxia [20% O_2]; $^{\#}p < 0.05$, $^{\#\#}p < 0.01$, as compared with the vehicle control in hypoxia [1% O_2]).

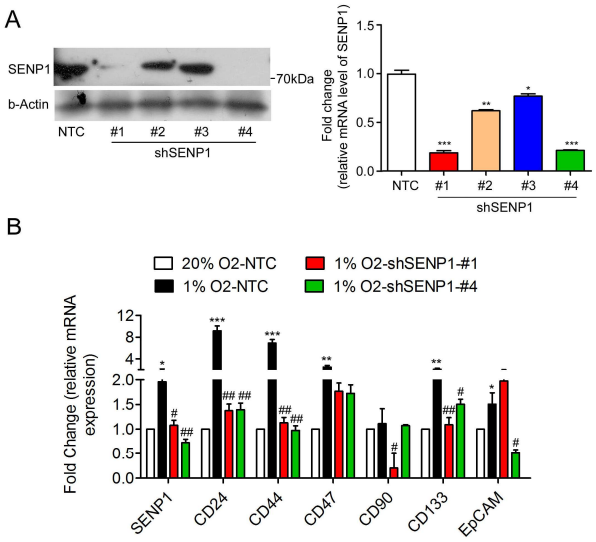

Figure S9. (A) SENP1 knockdown efficiency in MHCC-97L cells was examined by Western blot and q-PCR. (B) Expression of CD24, CD44, CD47, CD90, CD133 and EpCAM at mRNA levels was examined in HCC cells with SENP1 knockdown under hypoxia. (*$p < 0.05$, **$p < 0.01$, ***$p < 0.001$, as compared with the negative control in normoxia [20% O2]; $^{\#}p < 0.05$, $^{\#\#}p < 0.01$, $^{\#\#\#}p < 0.001$, as compared with the vehicle control in hypoxia [1% O2]).

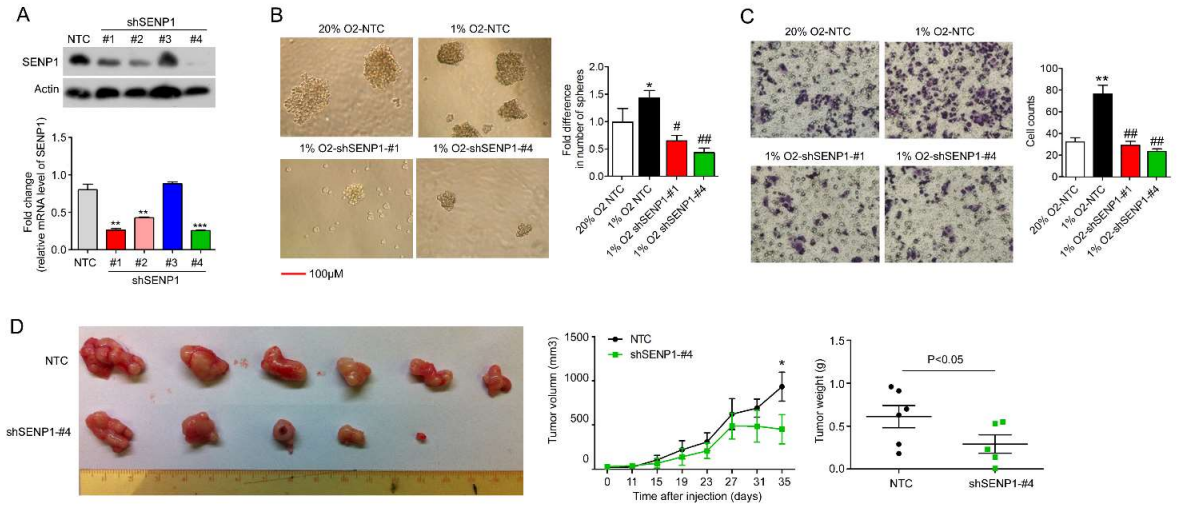

Figure S10. SENP1 knockdown suppressed cell growth of BEL-7402 cells under hypoxia both *in vitro* and *in vivo*. (A) Q-PCR and Western blots were used to examine the efficiency of stable SENP1 knockdown in BEL-7402. (B-C) Hypoxia-induced increase in self-renewal (B) and cell migration (C) was suppressed in two SENP1 knockdown BEL-7402 clones. (D) Xenograft model was performed in nude mice by subcutaneous injection of BEL-7402 cells with knockdown of SENP1 or NTC. (*$p < 0.05$, **$p < 0.01$, ***$p < 0.001$, as compared with the negative control in normoxia [20% O2]; $^{\#}p < 0.05$, $^{\#\#}p < 0.01$, $^{\#\#\#}p < 0.001$, as compared with the vehicle control in hypoxia [1% O_2]).

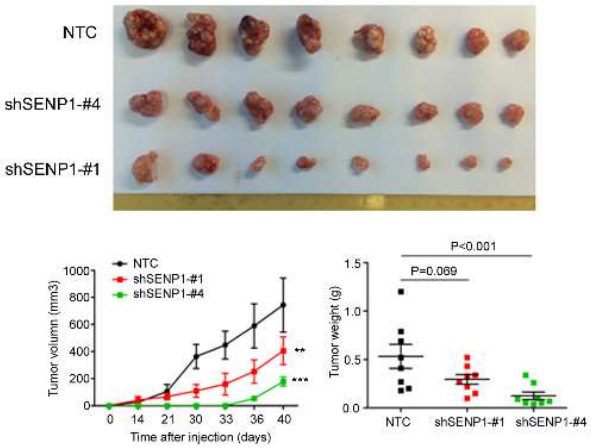

Figure S11. SENP1 knockdown suppressed cell growth of MHCC-97L *in vivo*. Xenograft model was performed in nude mice by subcutaneous injection of MHCC-97L cells with knockdown of SENP1 or NTC. (*p < 0.05, **p < 0.01, ***p < 0.001, as compared with negative control).

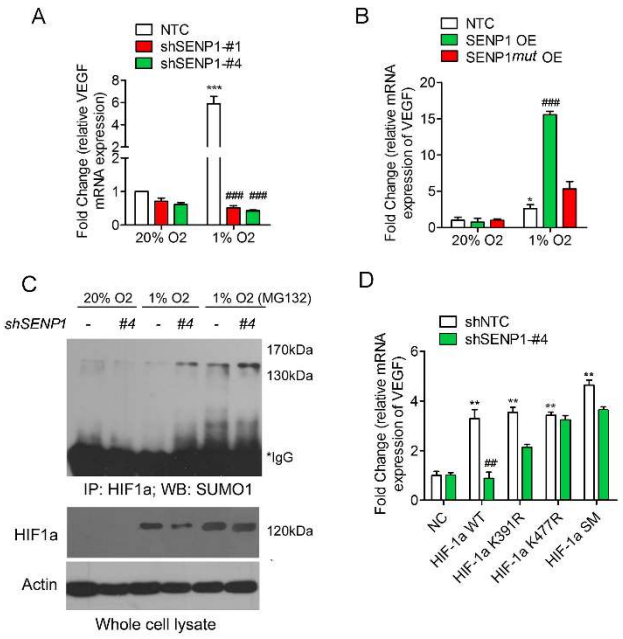

Figure S12. (A) Fold changes of the relative VEGF mRNA levels were examined by q-PCR in SENP1 knockdown and NTC SMMC-7721 cells after incubation under normoxia or hypoxia for 24 hr. (B) Fold changes of the relative VEGF mRNA levels were examined in NTC, SENP1 overexpression (SENP1 OE) and SENP1mut overexpression (SENP1m OE) Huh7 cells after incubation under normoxia or hypoxia for 36 hr. (C) Treatment with MG132 (proteasome inhibitor) resulted in the accumulation of SUMOylated HIF-1α and increased HIF-1α stabilization in HCC cells with SENP1 knockdown in hypoxia. Western blot and IP were performed to examine the protein levels of HIF-1α and SUMOylated HIF-1α. (D) Fold changes of the relative VEGF mRNA levels were examined in SENP1 knockdown and NTC SMMC-7721 cells, in which HA-SUMO-1 was co-transfected with RGS-HIF-1α WT, RGS-HIF-1α K391R, RGS-HIF-1α K477R, or RGS-HIF-1α SM.

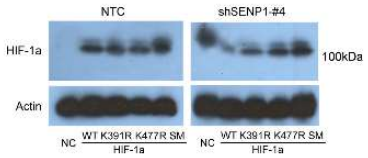

Figure S13. Western blots to detect the HIF-1a protein level in stable overexpressing HIF-1α WT, HIF-1α K391R, HIF-1α K477R or HIF-1α SM MHCC-97L with SENP1 or NTC knockdown.

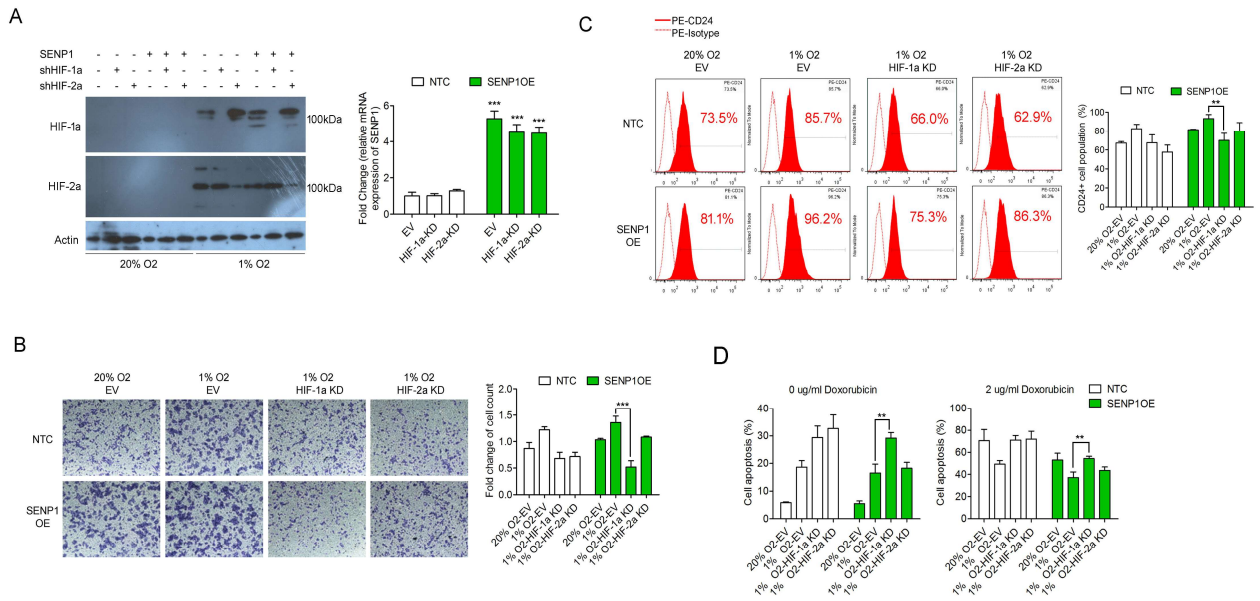

Figure S14. Effects of HIF-1α or HIF-2α knockdown on SENP1-enhanced stemness of Huh-7 cells in hypoxia. (A) Q-PCR and Western blots were used to detect the levels of SENP1 mRNA and HIF-1/2α in Huh7 cells. (B-D) Cell migration (B), chemoresistance (C) and $CD24^+$ cell population (D) were detected in hypoxia. (*$p < 0.05$, **$p < 0.01$, ***$p < 0.001$).

Table S1. Clinicopathological correlation of SENP1 expression in human HCCs.

Clinicopathological Features	No. of cases without SENP1 overexpression FC ≤ 4	No. of cases with SENP1 overexpression FC > 4	P value
Gender			
Male	32	40	0.343
Female	13	22	
Tumor size			
>5cm	31	17	0.565
<=5cm	48	14	
Tumor microsatellite formation			
Absent	24	12	0.408
Present	37	22	
Tumor encapsulation			
Absent	42	27	0.442
Present	19	7	
Venous invasion			
Absent	47	12	0.042*
Present	13	23	
Cellular differentiation			
Edmondson grade I-II	33	10	0.134
Edmondson grade III-IV	31	21	
TNM staging			
I-II	52	12	0.034*
III-IV	23	19	

* Chi-square test; FC, fold change.

Table S2. Limiting dilution data.

Huh7	cell number of injection	Huh7-NTC	Huh7SENP1 OE
Frequency	5000	0/6	3/6
	50000	2/6	6/6
	500000	4/6	6/6

Table S3. Confidence intervals for 1 / (stem cell frequency).

Huh7	Lower	Estimate	Upper	P value
NTC	834537	340389	138838	< 0.0001
SENP1OE	21410	7121	2369	

OE: overexpressing.

Table S4. Limiting dilution data.

MHCC-97L	cell number of injection	MHCC-97L-NTC	MHCC-97L-shSENP1
Frequency	100	5/6	2/6
	1000	5/6	3/6
	10000	6/6	5/6

Table S5. Confidence intervals for 1 / (stem cell frequency).

MHCC-97L	Lower	Estimate	Upper	P value
NTC	686	249	90.6	< 0.0001
shSENP1	7124	2722	1040.2	

Primer sequences for q-PCR analyses

Gene	*Forward primer (5'-3')*	*Reverse primer (5'-3')*	*GenBank No.*	*Ref*
SENP1	TTGGCCAGAGTGCAAATGG	TCGGCTGTTTCTTGATTTTTGTAA	NM_001267594	(1)
SENP1-HRE1	GACGTTCCTTAGTGCTGGCGGGTAGGTTTGA	GGCACCAAGTTTGTGGAGCTGAGAACGGG	/	(1)
SENP1-HRE2	TCCGTCCTCAAGTTGCTTGT	CGATCTCAGGCTATCTCGTGT	/	(1)
SENP1-HRE3	ATCCGTCCTCAAGTTGCTTGT	TCGATCTCAGGCTATCTCGTG	/	(1)
CD24	TGAAGAACATGTGAGAGGTTTGAC	GAAAACTGAATCTCCATTCCACAA	NM_013230	(2)
CD47	GGCAATGACGAAGGAGGTT	ATCCGGTGGTATGGATGAGA	NM_001777	(3)
CD44	CTGCCGCTTTGCAGGTGTA	CATTGTGGGCAAGGTGCTATT	NM_000610	(2)
CD90	GACAGCCTGAGAGGGTCTTG	CCCAGTGAAGATGCAGGTTT	NM_006288	(2)
CD133	TGGATGCAGAACTTGACAACGT	ATACCTGCTACGACAGTCGTGGT	NM_001145847	(2)
EpCAM	AATCGTCAATGCCAGTGTACTT	TCTCATCGCAGTCAGGATCATAA	NM_002354	(2)
VEGFa	GCAGAATCATCACGAAGTGG	GCATGGTGATGTTGGACTCC	NM_001171630	(1)
EPO	AAGGAGGCAGAAAATGTCACGATG	GTGAGTGTTCGGAGTGGAGCAGGT	NM_000799	(1)
LOX	GTTCCAAGCTGGCTACTC	GGGTTGTCGTCAGAGTAC	NM_002317	(1)
LOXL2	GGAAAGCGTACAAGCCAGAG	GCACTGGATCTCGTTGAGGT	NM_002318	(4)
NANOG	AATACCTCAGCCTCCAGCAGATG	TGCGTCACACCATTGCTATTCTTC	NM_024865	(4)
NOTCH1	CCTGAGGGCTTCAAAGTGTC	CGGAACTTCTTGGTCTCCAG	NM_017617	(2)
OCT3/4	CTTGCTGCAGAAGTGGGTGGAGGAA	CTGCAGTGTGGGTTTCGGGCA	NM_002701	(2)
SOX2	AAATGGGAGGGGTGCAAAAGAGGAG	CAGCTGTCATTTGCTGTGGGTGATG	NM_003106	(2)
BMI-1	TGGAGAAGGAATGGTCCACTTC	GTGAGGAAACTGTGGATGAGGA	NM_005180	(2)
ABCB1	AAATTGGCTTGACAAGTTGTATATGG	CACCAGCATCATGAGAGGAAGTC	NM_000927	(2)
ABCB5	TCTGGCCCCTCAAACCTCACC	TTTCATACCGCCACTGCCAACTC	NM_178559	(2)
ABCC1	CTCCTCCTATAGTGGGGACATCAG	GTAGTCCCAGTACACGGAAAG	NM_004996	(2)

ABCC2	ATGCAGCCTCCATAACCATGA	CTTCGTCTTCCTTCAGGCTATTCA	NM_000392	(2)
β-ACTIN	CATCCACGAAACTACCTTCAACTCC	GAGCCGCCGATCCACACG	NM_001101	(2)
HPRT1	CTTTGCTGACCTGCTGGATT	CTGCATTGTTTTCGGAGTGT	NM_000194	(2)

Experimental Procedures

Cell lines and culture.

Human HCC cell lines, BEL7402, Huh7, and SMMC-7721, were gifts from Shanghai Institute of Cell Biology, Chinese Academy of Sciences. Human HCC cell line, PLC/PRF/5, was from American Type Culture Collect (ATCC). Metastatic human HCC cell line, MHCC-97L, was gift from Fudan University (Dr. Z.Y. Tang) of Shanghai. Cells were maintained in DMEM with high glucose (Gibco BRL, Grand Island, NY) supplemented with 10% heat-inactivated fetal bovine serum (Gibco BRL), 100 mg/mL penicillin G, and 50 μg/mL streptomycin (Gibco BRL) at 37°C in a humidified atmosphere containing 5% CO2. Hypoxic environment was created by culturing cells in 1% O2/5% CO2/balance N2 in a modulator incubator chamber at 37°C.

Plasmids, constructs.

PcDNA3.1-SENP1 and pcDNA3.1-SENP1m constructs were subcloned from pTCP-SENP1 construct (transOMIC, Huntsville, AL, USA) and pFlag-CMV-SENP1m (Addgene) by BamHI and XhoI restriction enzymes (New England Biolabs). HA-SUMO-1, HA-SUMO-2 and HA-SUMO-3 were purchased in Addgene (Cambridge, MA, USA). RGS-HIF1α, RGSHIF1α K391R, RGS-HIF1α K477R, and RGS-HIF1α SM (K391R, K477R) were provided by Prof. Edward Yeh of University of Texas, Houston Health Science Center. The 6 X VEGF HRE promoter (VEGF-Luc) was generated as described in previous studies.

Transfection.

For transient transfection, Lipofectamine 2000 transfection reagent was used following manufacturer's protocol (Invitrogen). Lentiviruses were prepared by transient co-transfection with helper plasmids into 293T cells using Lipofectamine 2000.

Patient samples.

Human HCC and corresponding non-tumorous liver samples were collected at the time of surgical resection at Queen Mary Hospital, the University of Hong Kong. After collection from surgical resection, all samples were immediately snap-frozen in liquid nitrogen before storage at -80°C. Use of human samples was approved by the Institutional Review Board of the University of Hong Kong/ Hospital Authority Hong Kong West Cluster.

Clinical Characteristics of patients for prognostic analysis

The age of the patients ranged from 24 to 82 years, with a mean age of 51.4 years. There were 72 men and 35 women. Tumors were staged according to the pathological tumor-node-metastasis (pTNM) staging system, 1997 version.

Stable RNA interference.

Stable HCC clones that express shRNAs against HIF-1α, HIF-2α and non-target control (NTC) were generated as previously described [5]. SENP1 siRNAs were synthesized in LifeTech. The scramble sequence was used as a nonspecific siRNA control. The siRNA oligos were inserted into a pLKO.1 vector (Addgene) according to manufacturer's instructions. MHCC-97L and BEL-7402 cells were transfected with the siRNA plasmid using

lipofectamine 2000 (Invitrogen). Silencing efficiency of the siRNA was confirmed by performing real-time PCR to examine SENP1 expression. To establish HCC cell lines with stable SENP1 knockdown, lentiviral particles expressing shRNAs were packaged in 293T cells by transfection of pLKO.1-shSENP1 or NTC. MHCC-97L and BEL-7402 cells were infected by lentiviral particles and transduced cells were selected with 2 μg/mL puromycin.

Gene	***siRNA sequence***	***GenBank No.***
siSENP1-#1	CAAGAAGUGCAGCUUAUAATT	NM_001267594
siSENP1-#2	GCAGUGAAACGUUGGACAATT	NM_001267594
siSENP1-#3	AACTACATCTTCGTGTACCTC	NM_001267594
siSENP1-#4	CTAAACCATCTGAATTGGCTC	NM_001267594
shHIF-1α	GTTACGTTCCTTCGATCAG	NM_181054
shHIF-2α	CGACCTGAAGATTGAAGTGAT	NM_001430

Sphere formation assay.

A total of 200 single HCC cells were plated onto 24-well polyHEMA (Sigma)-coated plates. Cells were grown in DMEM/F12 medium (Invitrogen, Carlsbad, CA) for 10 days supplemented with 4 μg/mL insulin (Sigma-Aldrich, St. Louis, MO), B27 (Invitrogen, Carlsbad, CA), 20 ng/mL EGF (Sigma-Aldrich, St. Louis, MO), and 20 ng/mL basic FGF (Invitrogen, Carlsbad, CA).

Cell proliferation assay.

Cells were seeded at a density of 1,000 cells per well and allowed to grow for three to five days. Cell proliferation was assessed by a colorimetric assay using crystal violet as described previously [6].

Cell migration assays.

The migration assay was performed as described [7]. Photographs of five randomly selected fields of the fixed cells were captured and cells were counted. The experiments were repeated independently three times.

Annexin V staining.

Cells were stained in binding buffer, 7-AAD and FITC-conjugated Annexin V as provided by the Annexin-V-FLUOS Staining Kit (Roche Diagnostics) according to manufacturer's instructions. Analysis was determined by a FACSCalibur flow cytometer (BD Biosciences).

Cell sorting.

Viable $CD24^-$ and $CD24^+$ cells from a single cell suspension of MHCC-97L were sorted using a FACSAria cell-sorter equipped with an automated cell deposition unit (ACDU) and using 488-nm laser light. For single cell deposition, cells were sorted using the 70μm nozzle with the sheath pressure set at 70 PSI using the sort precision mode set at single cell. Dead cells were excluded from the sort based on their forward and side scatter characteristics using an electronic gate, before applying sort gates to define $CD24^+$ expressing cells for collection. Sorted cells were seeded in 6-well plates with 1×10^5 cells per one well. Plates were

maintained at 37°C in a humidified incubator with 5% CO2 in either hypoxia or normoxia.

Flow cytometric analysis.

Phycoerythrin (PE)-conjugated CD24 (BD PharMingen, San Jose, CA) was used in the experiment. Cells were incubated in phosphate-buffered saline (PBS) containing 2% fetal bovine serum (FBS) followed by PE-conjugated antibodies. Isotype-matched mouse immunoglobulins served as controls. The samples were analyzed using FACSCanto II analyzer flow cytometer (BD Biosciences, San Jose, CA).

Chromatin immunoprecipitation (ChIP) assay.

MHCC-97L cells were cross-linked with formaldehyde, lysed with SDS buffer, and sonicated. Sheared DNA was precleared with salmon sperm DNA/protein A agarose slurry (Merck Millipore) and immuno-precipitated with HIF-1α, HIF-2α, HIF-1β and IgG (Santa Cruz). Agarose beads were incubated with antibody/protein/DNA complex and washed with low-salt buffer, high-salt buffer, and LiCl wash buffer according to manufacturer's protocol (Millipore). DNA was eluted in 1%SDS/0.1M NaHCO3, de-cross-linked with NaCl (0.2M), and extracted by phenol-chloroform. For qPCR analysis of the ChIP samples, purified immunoprecipitates were dissolved in 50 μL of water. Standard PCR reactions using 3μL of the immunoprecipitated DNA were performed with a SYBR Green PCR kit (Applied Biosystems) using primers for SENP1-HRE.

Quantitative PCR (q-PCR) analysis.

Total RNA was isolated using Trizol reagent according to the manufacturer's protocol (Invitrogen, Carlsbad, CA). Complementary DNA (cDNA) was synthesized using a GeneAmp® Gold RNA PCR Kit (Applied Biosystems, Foster City, CA) according to the manufacturer's instructions and then subjected to PCR with a SYBR Green PCR kit with primers (the sequences are provided in the Supplementary table1). The amplification protocol consisted of incubations at 94°C for 15 seconds, 63°C for 30 seconds, and 72°C for 60 seconds. Incorporation of the SYBR Green dye into PCR products was monitored in real time with an ABI 7900HT Sequence Detection System and SDS 1.9.1 software (Applied Biosystems) and subsequently analyzed using RQ Manager 1.2 software (Applied Biosystems), thereby allowing the threshold cycle (CT) at which exponential amplification of the products began to be determined. The amount of target cDNA was calculated relative to that of β-actin or HPRT cDNA.

Immunostaining

For paraffin-embedded tissues, sections were deparaffinized in xylene and rehydrated in graded alcohols and distilled water. Slides were processed for antigen retrieval by a standard microwave heating technique. Specimens were incubated with goat anti-human SENP1 (HPA011765, Atlas Antibodies AB, Sweden) in a dilution of 1:60. Subsequent immunodetection was performed using the standard rapid EnVision technique. The reaction was then developed with the DAKO Liquid DAB_Substrate-Chromogen System (DAKO, Carpentaria, CA). Sections were counterstained with Mayer's hematoxylin. Stained slides were imaged on an Aperio Scanscope® CS imager (Vista, CA), generating 0.43 μm/pixel

whole slide images.

Western blot analysis.

Total protein extracted from HCC cells was separated with SDS-PAGE and transferred to PVDF membrane. The primary antibodies included rabbit anti-human SENP1, HIF-1α, HIF-2α, SUMO1, SUMO2/3 (Abcam, Cambridge, MA), mouse anti-human β-actin (Santa Cruz Technology, Santa Cruz, CA) and anti-HA tag (Roche). After washing, the membrane was incubated with horseradish peroxidase–conjugated anti-mouse or rabbit (Amersham) and then visualized by enhanced chemiluminescence plus according to the manufacturer's protocol.

Immunoprecipitation.

For detecting the SUMOylation of HIF-1α and HIF-2α in HCC cells, 2×10^6 cells were harvested with immunoprecipitation lysis buffer (20 mM Tris-HCl, pH 7.6; 300 mM NaCl; 1 mM EDTA; 1% NP-40; 10% glycerol; 20 mM N-ethyl-maleimide (NEM); 1 mM PMSF; protease inhibitor cocktail). After brief sonication, the lysates were centrifuged (17,000 g, 15 min) at 4 °C. After pre-clearing with normal IgG at 4 °C for 2 hrs, supernatants were incubated with antibody against HIF-1α (ab463, Abcam, Cambridge, MA) or HIF-2α (ab199, Abcam, Cambridge, MA) together with protein A plus-agarose (Santa Cruz, CA) overnight at 4 °C. After immunoprecipitation, the beads were washed five times with washing buffer (50 mM Tris-HCl, pH 7.6; 300 mM NaCl; 1 mM EDTA; 0.5% NP-40; 10% glycerol), then precipitates were analyzed by Western blot with antibody against SUMO1 or SUMO2/3

(Abcam, Cambridge, MA). For detecting the binding of exogenous HIF-1α and SUMO1 in HCC cells and determining the SUMO site of HIF-1α in HCC cells, RGS-HIF1α, RGSHIF1α K391R and RGS-HIF1α K477R were co-transfected with HA-SUMO1 into SMMC7721 cells with stable SENP1 knockdown or NTC. Twenty-four hours after transfection, cells were harvested with SUMOylation lysis buffer, and IP and WB were conducted with antibody against HIF-1α and HA respectively.

Luciferase reporter assay.

HCC cells were seeded in a 12-well plate and transfected with indicated plasmids and pGL3-HRE-luciferase (Luc) (200 ng), a luciferase reporter construct containing six HREs of the promotor of VEGF gene together with pSV40-renilla (10 ng). The empty vectors were supplemented to 750 ng of the total plasmid concentration. Then cells were culture in hypoxia or normoxia or HIF-1α and the SUMO site mutant constructs was transfected into the cells on day 2. 24hr later, luciferase signals were detected by Dual-Luciferase® Reporter Assay (Promega) on day 3. The relative Luc activity was normalized by renilla activity.

Animal Experiments

Animal care and experiments were performed in strict accordance with the “Guide for the Care and Use of Laboratory Animals’’ and the ‘‘Principles for the Utilization and Care of Vertebrate Animals’’ and were approved by the Experimental Animal Ethical Committee at Li Ka Shing Faculty of Medicine, The University of Hong Kong. Different numbers of cells were injected subcutaneously into nonobese diabetic (NOD)/ severe combined

immunodeficient SCID mice. Three dimensions of tumors were measured with caliper weekly and tumor volume was calculated with formula: length x width x depth x 0.52 (mm3).

Reference:

1. Xu Y, Zuo Y, Zhang H, Kang X, Yue F, Yi Z, et al. Induction of SENP1 in endothelial cells contributes to hypoxia-driven VEGF expression and angiogenesis. J Biol Chem 2010; **285**: 36682-8.

2. Lee TK, Castilho A, Cheung VC, et al. CD24 (+) liver tumor-initiating cells drive self-renewal and tumor initiation through STAT3-mediated NANOG regulation. Cell Stem Cell 2011; **9**:50-63.3.

3 Lee TK, Cheung VC, Lu P, Lau EY, Ma S, Tang KH, et al. Blockade of CD47-mediated cathepsin S/protease-activated receptor 2 signaling provides a therapeutic target for hepatocellular carcinoma. Hepatology 2014;60:179-91.

4. Wong CC, Tse AP, Huang YP, Zhu YT, Chiu DK, Lai RK, Au SL, Kai AK, Lee JM, Wei LL, Tsang FH, Lo RC, Shi J, Zheng YP, Wong CM, Ng IO. Lysyl oxidase-like 2 is critical to tumor microenvironment and metastatic niche formation in hepatocellular carcinoma. Hepatology 2014; **60**:1645-58.

5. Lai RK, Xu IM, Chiu DK, Tse AP, Wei LL, Law CT, Lee D, Wong CM, Wong MP, Ng IO, Wong CC. NDUFA4L2 fine-tunes oxidative stress in hepatocellular carcinoma. Clin Cancer Res 2016; **22**: 3105-17.

6. Ng, IO, Liang ZD, Cao L, Lee TK. DLC-1 is deleted in primary hepatocellular carcinoma and exerts inhibitory effects on the proliferation of hepatoma cell lines deleted

DLC-1. Cancer Res 2000; **60**: 6581-6584.

7. Wong CM, Yam JW, Ching YP, Yau TO, Leung TH, Jin DY, Ng IO. Rho GTPase-activating protein deleted in liver cancer suppresses cell proliferation and invasion in hepatocellular carcinoma. Cancer Res 2005; **65**: 8861-886